

ARMY RESEARCH LABORATORY



3-D Holographic Display Using Strontium Barium Niobate

by Christy A. Heid, Brian P. Ketchel, Gary L. Wood,
Richard J. Anderson, and Gregory J. Salamo

ARL-TR-1520

February 1998

DTIC QUALITY INSPECTED 2

19980305 054

Approved for public release; distribution unlimited.

The findings in this report are not to be construed as an official Department of the Army position unless so designated by other authorized documents.

Citation of manufacturer's or trade names does not constitute an official endorsement or approval of the use thereof.

Destroy this report when it is no longer needed. Do not return it to the originator.

Army Research Laboratory

Adelphi, MD 20783-1197

ARL-TR-1520

February 1998

3-D Holographic Display Using Strontium Barium Niobate

Christy A. Heid, Brian P. Ketchel, Gary L. Wood
Sensors and Electron Devices Directorate, ARL

Richard J. Anderson
National Science Foundation

Gregory J. Salamo
University of Arkansas

Abstract

An innovative technique for generating a three-dimensional holographic display using strontium barium niobate (SBN) is discussed. The resultant image is a hologram that can be viewed in real time over a wide perspective or field of view (FOV). The holographic image is free from system-induced aberrations and has a uniform, high quality over the entire FOV. The enhanced image quality results from using a phase-conjugate read beam generated from a second photorefractive crystal acting as a double-pumped phase-conjugate mirror (DPPCM). Multiple three-dimensional images have been stored in the crystal via wavelength multiplexing.

Contents

1. Introduction	1
2. Theory	2
3. Experimental Setup	5
3.1 Holographic Display	6
3.2 Image Storage	9
4. Conclusions	11
Acknowledgements	11
References	12
Distribution	13
Report Documentation Page	17

Figures

1. Dynamic holography in photorefractive crystals via four-wave mixing	2
2. Experimental setup used to record and reconstruct a 3-D hologram using SBN	5
3. 3-D hologram stored in a Ce-doped SBN:60 photorefractive crystal and viewed at various angles with an FOV of $\sim 14^\circ$	7
4. Method of measuring expected FOV for recording a hologram in a crystal of length L_c	7
5. Hologram stored in a mosaic of two Ce-doped SBN:60 photorefractive crystals with an FOV of $\sim 30^\circ$	8

Tables

1. Relative powers of writing and reading beams used to study wavelength multiplexing in SBN	9
--	---

1. Introduction

Present holographic displays, such as those generated by computers or emulsion films, usually require intermediate preprocessing or post-processing and are, therefore, not capable of real-time production and viewing and have limited information storage capacity. The use of photorefractive crystals, such as strontium barium niobate (SBN), as a holographic storage medium eliminates these and other limiting factors. For example, when a photorefractive storage medium is used, holograms may be recorded and projected without time-consuming processing and with greater storage capacity through various forms of multiplexing. Additionally, the photorefractive recording medium is sensitive to low level intensity and is reusable. Therefore, previously stored holograms may be erased, and the crystal can be reused to store other holograms. Until recently, however, research in photorefractive holography has been limited to the production of two-dimensional (2-D) holograms and very limited field-of-view (FOV) 3-D holograms.

The proposed method employs a volume hologram recorded and read in real time in a photorefractive crystal to produce a 3-D image. This innovative technique is simple, and it differs from previous attempts at 3-D displays. We used a photorefractive material, SBN, to record a hologram, and a phase-conjugate read beam, which is generated from a double-pumped phase-conjugate mirror (DPPCM), to accurately reproduce the holographic image in space over a large perspective. The resultant holographic image is free from system-induced aberrations, may be viewed over a wide range of angles that can be expanded by the use of a mosaic of crystals, and has uniform high quality over the entire FOV.

2. Theory

The hologram is recorded in SBN by the interference of two writing beams: a reference beam E_{ref} and an object beam E_o , as shown in figure 1. The intensity that is created by the interference of the two writing beams, E_{ref} and E_o , is written as

$$I \propto (E_{ref} + E_o)(E_{ref}^* + E_o^*) = |E_{ref}|^2 + |E_o|^2 + E_{ref}E_o^* + E_oE_{ref}^* \quad (1)$$

where the grating terms of the intensity are represented by the last two terms

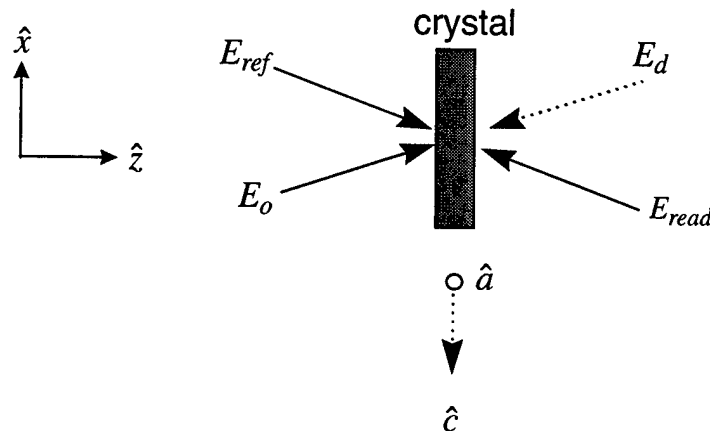
$$I_g = E_{ref}E_o^* + E_oE_{ref}^* \quad (2)$$

When two coherent beams interfere in a photorefractive crystal such as SBN, an index-of-refraction grating is produced via the photorefractive effect [1]. The gratings are written on the order of the photorefractive time response, which can be less than 1 s. The time response for these crystals is intensity dependent, $\tau = A/I$ with $0.05 < A < 2 \text{ J/cm}^2$, depending on crystal and dopant type and quality.

The photorefractive effect occurs when two beams of the same frequency interfere so that a series of light and dark fringes is created by the constructive and destructive interference of the beams. In the light or high-intensity regions, free charge carriers are excited by photons into the conduction band. These charge carriers diffuse into the darker regions of lower intensity. Once this process occurs, the charge carriers become trapped, which induces a space-charge distribution. As stated in Poisson's equation, a space-charge field results from the space-charge distribution. This space-charge field then induces an index grating, via the linear electro-optic, known as the Pockels effect

$$\Delta n = -\frac{1}{2} n^3 r_{eff} E_{sc} \quad (3)$$

Figure 1. Dynamic holography in photorefractive crystals via four-wave mixing; \hat{c} -axis is drawn for a photorefractive crystal such as SBN.



where n is the index of refraction, r_{eff} is the effective electro-optic coefficient, and E_{sc} is the strength of the space-charge field.

With no applied or photovoltaic electric field, the index-of-refraction grating is phase shifted by 90° from the intensity grating, which leads to energy exchange between the two beams. Energy exchange leads to significant beam fanning if there is sufficient interaction length in the crystal. Beam fanning is undesirable for the holographic storage crystal because it will degrade the hologram. Therefore, the crystal used in this study, SBN doped with cerium, had a length of ~ 1 mm, which is less than the critical interaction length.

The hologram is read by the introduction of a third beam E_{read} , which is counter-propagating to the reference beam as shown in figure 1. The read beam is diffracted off the index grating, which has been previously recorded in the photorefractive material. This process produces the diffracted wave E_d and is written as

$$E_d \propto E_{read} I_g = E_{read} (E_{ref} E_o^* + E_o E_{ref}^*) = E_{ref} E_o^* E_{read} + E_o E_{ref}^* E_{read} \quad , \quad (4)$$

where I_g is defined in equation (2). The first term on the right-hand side of the equation, $E_{ref} E_o^* E_{read}$, represents a beam that is diffracted off the index grating, counter-propagating to the object beam, with wave vector $k_{d1} = -k_o$.

The second term, $E_o E_{ref}^* E_{read}$, represents a beam propagating with wave vector $k_{d2} = k_o - 2k_{ref}$. Only the first-order wave k_{d1} will be Bragg-matched [2], because we are in the thick or volume grating regime. We are in the thick (volume) grating regime because the following inequality is satisfied:

$$2\pi\lambda d \gg n\Lambda^2 \quad , \quad (5)$$

where λ is the wavelength in free space, d is the grating thickness, n is the average index of refraction, and Λ is the grating period.

There are several advantages to using volume holograms over those recorded in the thin grating regime. First, the diffraction efficiency of volume gratings is significantly greater than what is offered by thin gratings because a volume grating has fewer diffracted orders. Thus, only a single beam is diffracted from the grating, which eliminates the appearance of ghost images due to higher order diffraction. Second, there is less angular spread in the diffracted beam as compared to the beam from a thin grating. This feature allows numerous holograms to be written and read in the same crystal, because the Bragg angle is used to selectively store and read the images. Finally, only light that is incident at the narrow Bragg angle can be diffracted by these gratings, which minimizes crosstalk during volume readout.

A simple method of reading the hologram involves using the reflection of the reference beam from a plane mirror. The generated diffracted beam is written as follows, where equation (4) is used for a volume grating:

$$E_d \propto E_o^* E_{ref} E_{read} = r A_{read}^2 e^{2ik_x x} E_o^* \quad , \quad (6)$$

where $E_{read} = r E_{ref}$, $E = A e^{ik_x x + ik_z z}$ (such that the beam is propagating in the $\hat{x} - \hat{z}$ plane with wave vector k and amplitude A), and r is the reflection coefficient of the plane mirror.

The image-bearing beam E_d contains a spatially dependent term because the read beam is only truly phase-matched on axis. Thus, the maximum FOV of the hologram is severely restricted as the read beam diverges. This problem can be remedied by careful collimation of the read beam and reference beam; however, this is a cumbersome task. It is much easier to use the laws of nonlinear optics and use a read beam that is naturally self-aligning, such as a phase-conjugate read beam. Since the phase-conjugate beam is exactly counter-propagating to the reference beam, it would not matter if the reference beam is diverging because the read beam will retrace its path precisely, and read all the written gratings over the entire beam width. The read beam, which is generated from the phase conjugate of the reference beam, is written as follows, where equation (4) is used for a volume grating:

$$E_d \propto E_o^* E_{ref} E_{read} = q |E_{ref}|^2 E_o^* \propto q I_{ref} E_o^* = \sqrt{I_{ref} I_{read}} E_o^* \quad , \quad (7)$$

where $E_{read} = q E_{ref}^*$ and q is the phase-conjugate reflectivity.

The divergence of the read beam from a plane mirror, evident in equation (6), is not present when a phase-conjugate read beam is used, as shown in equation (7). Furthermore, phase conjugation is a process in which the phase aberrations of an optical system are removed without beam manipulation. The use of a phase-conjugate read beam also has added benefits such as higher resolution, a larger FOV, and a simpler, more robust holographic production [3].

Phase conjugation at low beam powers can be obtained by the use of photorefractive crystals [4] and generated by four-wave mixing geometries [5]. One method, which uses the internal reflection of one beam within the crystal, is called self-pumped phase conjugation. The self-pumped, phase-conjugate mirror offers reflectivities in the range of $0 \leq q \leq 1$. However, reflectivities greater than 1 can be achieved by the use of a DPPCM. We used the photorefractive crystal SBN doped with cerium as a DPPCM. The bridge-conjugator geometry was used to generate the phase-conjugate read beam because a large gain in SBN is easier to achieve [6]. In the bridge conjugator geometry, the reference and pump beams are incident on opposite faces of a photorefractive crystal, which are parallel to the \hat{c} -axis. Since the pump beam does not have to be mutually coherent with the reference beam, the pump beam can be generated from the original laser or a second laser operating at the same wavelength. Actually, the DPPCM is more efficient when the beams are not coherent.

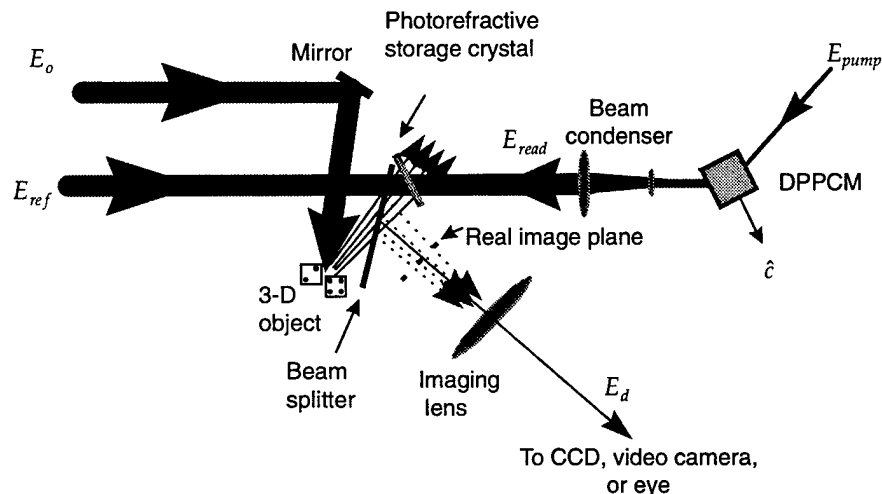
3. Experimental Setup

The basic principles upon which this three-dimensional display operates are shown in figure 2. A signal beam, generated from an argon-ion laser operating at 488 nm, is split into two beams: the object beam (E_o) and reference beam (E_{ref}). A delay arm was placed in the reference beam path to adjust the coherence between the two writing beams. The coherence length of the argon laser was measured to be ~ 70 mm. To obtain the maximum allowable FOV of the hologram, it is desirable to completely fill the photorefractive crystal that is being used as the recording medium. Therefore, a beam expander is used to increase the reference beam diameter and to collimate it before it enters the recording medium. The object beam is incident on the object at an angle, so that the majority of the scattered light is directed towards the recording medium. Depending on the size of the object, the object beam may need to be expanded. The scattered object beams and reference beam cross and interfere in the recording medium. In this study, the recording material was a photorefractive crystal (strontium barium niobate $Sr_{0.6}Ba_{0.4}Nb_2O_6$ (SBN:60)), which was doped with cerium.

The angle between the reference and object beams was made to correspond with the largest change in the index of refraction. We performed two beam coupling experiments on SBN:60 to determine the angle that achieved the strongest possible photorefractive effect. The optimum angle for SBN:60 was measured to be within 20° to 40° , and the bisector of this angle was normal to the incident face of the crystal.

The entrance and exit faces of the crystal were cut parallel to the direction of the largest electro-optic coefficient (r_{33} for SBN:60), which was labeled the \hat{c} -axis. The crystal was electrically poled in this same direction to ensure domain alignment. The \hat{c} -axis should lie in the plane of polarization of the object and reference beams; therefore, \hat{p} -polarized light was used in this study. The entrance and exit faces of the crystal should also be as large as possible to maximize the FOV, and the crystal thickness should be about 1 mm to minimize the effects of beam fanning (discussed previously). The dimensions of the photorefractive storage crystal used in this study were $20 \times 20 \times 1.3$ mm.

Figure 2.
Experimental setup
used to record and
reconstruct a 3-D
hologram using SBN.



The hologram recording process occurs wherever the reference beam and scattered object beams intersect in the crystal volume. As long as these beams are mutually coherent and the photorefractive material has sufficient response, interference will occur, which will result in an intensity modulation. These interference gratings transform into index-of-refraction gratings via the photorefractive effect that was discussed previously. The object is recorded as a conglomeration of index gratings in the crystal volume, which is referred to as a volume hologram.

After the reference beam transmits through the storage crystal, it is incident upon a second photorefractive crystal that is used as a DPPCM. The DPPCM crystal, which is used to obtain the necessary phase-conjugate read beam, has parameters identical to the storage crystal except for the dimensions. In our experiment, the DPPCM SBN:60 crystal is 6 mm long, which provides a sufficient path length for significant beam fanning. Since the reference beam may be too large in diameter to enter the DPPCM crystal cleanly, a beam condenser is used. The beam condenser ensures that the desired beam size is achieved at the entrance face of the crystal. The DPPCM crystal is oriented so that the reference beam (E_{ref}) and a second pump beam (E_{pump}) enter opposite faces of the crystal with wave vector components in the $+\hat{c}$ -direction. The pump beam, which was \hat{p} -polarized, originated from a second argon-ion laser, which was operating at 488 nm.

The read beam (E_{read}) will exactly retrace the original beam's path from the DPPCM crystal—through any lenses—to the storage crystal. The read beam is counter-propagating to the reference beam in the storage crystal. Consequently, the read beam is perfectly Bragg-matched to the hologram's gratings at all points in the crystal. The exact match ensures that all gratings or holograms are read and allows the maximum perspective (FOV) of the image for the size of the storage material. Since the read beam is a phase conjugate, any inhomogeneities or phase-distorting properties of the optical elements between the DPPCM crystal and the hologram will cancel out. The Bragg-matched read beam will diffract off these gratings and retrace the path of the scattered object beam. The diffracted beam from the storage crystal is separated from the object beam by a beam splitter with an antireflection coating that is placed between the object and storage crystal. This process forms the three-dimensional hologram of the object as shown in figure 2.

3.1 Holographic Display

The three-dimensional hologram is a real image of the object and can be displayed in free space. The image can be viewed by projection, via lens relays, directly into the eye or a camera. Figure 3 shows the hologram of two dice earrings recorded in the SBN:60 photorefractive crystal. The dice have dimensions of 2 mm on a side. We verified the third dimension of the image by viewing the hologram at different perspectives, which demonstrated parallax when we rotated the viewing angle by placing the camera on a pivot arm. The FOV of the hologram (fig. 3) was measured to be $\sim 14^\circ$. We determined the FOV by the angular range in which the hologram was

clearly visible. The expected FOV can be calculated from the diagram shown in figure 4. The photorefractive recording crystal of length L_c is tilted so that the normal to the crystal's largest face bisects the angle between the reference and object beams, ϕ . The object of width s is located a distance d from the projection of the recording crystal, where the projection of the crystal is in the plane perpendicular to \bar{d} . The effective length of the recording material is

$$L_{eff} = L_c \cos\left(\frac{\phi}{2}\right) - s \quad , \quad (8)$$

where $L_c \cos(\phi/2)$ is the projection of the crystal to the plane normal to \bar{d} , and the object size is subtracted so that the entire object is observed through the FOV. The maximum FOV of the hologram is limited by the angular range over which the object can be viewed through the crystal. The FOV is calculated as follows:

$$FOV = 2 \arctan\left(\frac{L_{eff}}{2d}\right) \quad , \quad (9)$$

where L_{eff} is defined in equation (8) and d is the distance from the object to the projection of the recording crystal as shown in figure 4.

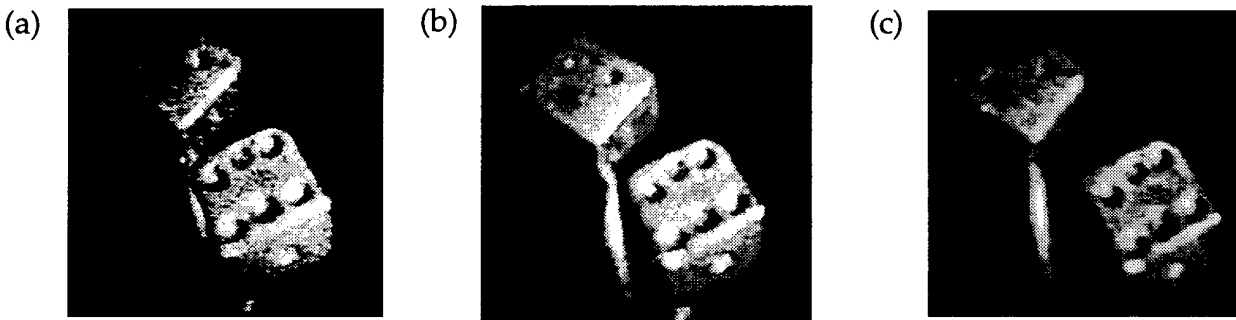
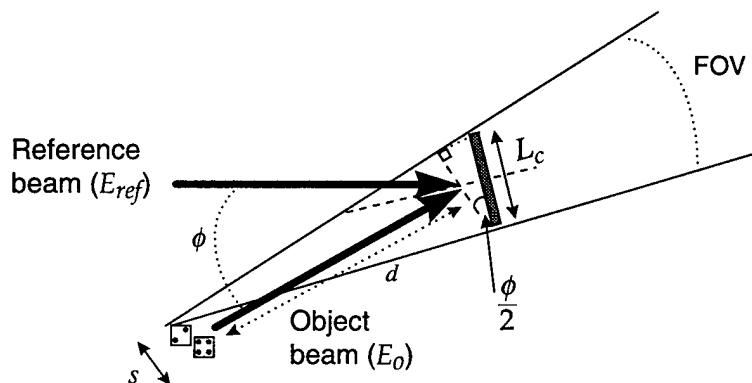


Figure 3. 3-D hologram stored in a Ce-doped SBN:60 photorefractive crystal and viewed at various angles with an FOV of $\sim 14^\circ$.

Figure 4. Method of measuring expected FOV for recording a hologram in a crystal of length L_c .

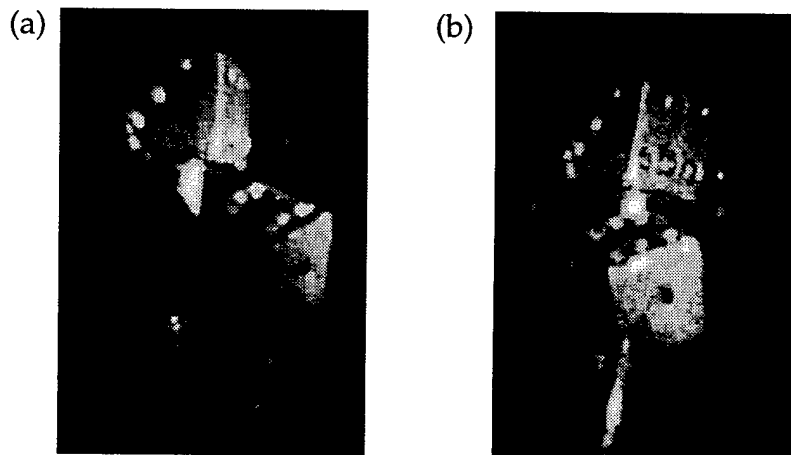


Using equations (8) and (9), we calculated the maximum FOV of the hologram presented in figure 3 to be $\sim 24^\circ$, where $L_c = 20$ mm, $d = 40$ mm, $\phi = 20^\circ$, and $s = 3$ mm. Because of incomplete phase conjugation of the read beam, the measured FOV of 14° is much less, because the entire region of the crystal was not used. The alignment of the pump beam and reference beam in the DPPCM is critical to enhance a large phase-conjugate read beam.

We used a second, identical photorefractive storage crystal (SBN:60 doped with cerium with similar dimensions (20 mm \times 20 mm \times 1.3 mm)) to further increase the FOV of the hologram. The two storage crystals were tiled together in a mosaic so that the width of the net storage area was 40 mm and the height was 20 mm. To produce a collimated reference and read beam with an elliptical shape that filled the rectangular-shaped storage crystal, we used a series of spherical and cylindrical lenses. A laser aplanatic lens and an aplanatic meniscus lens from CVI Laser Corporation were used to obtain an f number of $f/3.3$ to reduce distortions when the reference beam was focused into the DPPCM, and the read beam was expanded to fill the storage crystal. The hologram recorded in the mosaic of the two crystals is shown in figure 5. The increased perspective (FOV) is evident on the die in the background of figure 5, where the side of the die with the three is visible at one edge of the FOV, as shown in figure 5a; while at the other edge of the FOV, the side of the die with the six is clearly visible, as shown in figure 5b. We measured the FOV of the hologram presented in figure 5 to be $\sim 30^\circ$ by rotating the camera on a pivot arm that was centered at the image plane. The hologram is clearly visible through the entire FOV; however, there was a bright strip of light that appeared due to scattering when the viewing angle passed through the intersection where the two crystals were attached by double-sided tape. Using equations (8) and (9), we calculated the maximum FOV to be $\sim 44^\circ$, where $L_c = 40$ mm, $d = 45$ mm, $\phi = 20^\circ$, and $s = 3$ mm. As previously stated, the FOV was limited because the read beam did not fill the entire crystal. The maximum possible FOV is desired so that the images are more realistic.

We would also like to display the hologram in such a medium that the image could be viewed at different angles. A scattering liquid was tested, but proved ineffective since the perspective was lost, and only a 2-D image was visible.

Figure 5. Hologram stored in a mosaic of two Ce-doped SBN:60 photorefractive crystals with an FOV of $\sim 30^\circ$.



3.2 Image Storage

Presently, much research is focused on studying holographic storage in photorefractive crystals via angular [7], wavelength [8], and electric-field [9] multiplexing; however, these images are generally 2-D. We have stored multiple 3-D holograms in the photorefractive crystal via wavelength multiplexing. The experimental setup used to study wavelength multiplexing is shown in figure 2. However, the writing beams originated from an argon-ion laser that was operating in a multiline configuration. Also, the DPPCM was not used. The read beam was generated from a second argon-ion laser running in a single-line configuration. Several holograms were written simultaneously at the lasing wavelengths of the argon-ion laser.

The relative powers of the primary lasing wavelengths used to record the holograms are listed in table 1. We read the individual holograms by tuning the read beam to a particular wavelength. The relative powers of the read beam used to reconstruct individual holograms are also listed in table 1.

The holograms were clearly visible at each wavelength. Band pass filters were used to shield unwanted scattered light from writing-beam wavelengths that were not being read. We verified the three-dimensionality of the hologram by demonstrating parallax, as previously shown in figures 3 and 5.

Permanent storage of holographic images in photorefractive crystals is often obtained by electrical [10] or thermal [11] fixing of the gratings or by periodic refreshing [12]. However, we have found that the holograms persist without any external fixing mechanisms.

To study this effect, we used the experimental setup shown in figure 2 with the following changes: the beam splitter was removed so that the image was viewed in the same plane as the object, and the DPPCM was not used. The read beam was blocked while the hologram was recorded for approximately 5 min at a power of ~5 mW. Next, the recording beams were blocked, and the object, a dime, was removed so that the holographic image could be viewed. The hologram was reconstructed with a weaker read beam of ~0.8 mW. The hologram was quite bright, with a diffraction efficiency of ~3 percent, and persisted during readout for approximately 30 min without any apparent degradation. The holograms' long storage times, achieved without any external fixing mechanisms, could have arisen from self-enhancement [13].

Table 1. Relative powers of writing and reading beams used to study wavelength multiplexing in SBN.

Wavelength (nm)	Relative beam power	
	Writing	Reading
476.5	0.29	1
488	0.76	1
496.5	0.29	0.33
501.7	0.18	0.33
514.5	1	1

A hologram was also recorded in a photorefractive storage crystal for ~ 5 min; then, it was placed in a sealed, dark box for three days. The hologram was reconstructed after three days with a read beam of ~ 1.7 mW, and the hologram was still quite bright. Since external light will slowly erase the grating in the crystal, we turned off the room lights during these measurements.

4. Conclusions

A simple method for recording a real-time, 3-D hologram using SBN has been demonstrated. The 3-D hologram is a realistic image that can be viewed over a large FOV. A DPPCM was used to produce a phase-conjugate read beam in order to view the hologram over the maximum perspective (FOV). We further increased the FOV of the hologram by storing the hologram in a mosaic of two SBN crystals. Multiple 3-D images have been stored and read out of the crystal via wavelength multiplexing. The holograms were also noted to persist without any external fixing mechanisms. During readout, the holograms persisted for hours. When the photorefractive storage crystal was kept in a dark environment, the holograms persisted for days.

Acknowledgements

The principal author is on a fellowship appointment from the American Society for Engineering Education, Washington, DC, for the U.S. Army Research Laboratory. The authors wish to thank R. R. Neurgaonkar from Rockwell International Science Center, Thousand Oaks, CA, for supplying the photorefractive crystals.

References

1. R. W. Boyd, *Nonlinear Optics*, Academic Press, San Diego (1992), ch 10.
2. H. Kogelnik, "Coupled wave theory for thick hologram gratings," *Bell Syst. Tech. J.* **48**, No. 9 (November 1969), 2909–2947.
3. B. P. Ketchel, G. L. Wood, R. J. Anderson, and G. J. Salamo, "Three-dimensional image reconstruction using strontium barium niobate," *Appl. Phys. Lett.* **71**, No. 27 (2–4 July 1997).
4. P. Gunter, "Holography, coherent light amplification and optical phase conjugation with photorefractive materials," *Physics Reports*, North Holland Publishing Co., Amsterdam (1982).
5. G. L. Wood, W. W. Clark, M. J. Miller, G. J. Salamo, E. J. Sharp, R. R. Neurgaonkar, and J. R. Oliver, "Photorefractive materials," *Spatial Light Modulator Technology, Materials, Devices, and Applications*, U. Efron, ed., Marcel Dekker, Inc., New York (1995).
6. E. J. Sharp, W. W. Clark, M. J. Miller, G. L. Wood, B. Monson, G. J. Salamo, and R. R. Neurgaonkar, "Double phase conjugation in tungsten bronze crystals," *Appl. Opt.* **29**, No. 6 (1990), 743–749.
7. F. H. Mok, M. C. Tachitt, and H. M. Stoll, "Storage of 500 high-resolution holograms in a LiNbO_3 crystal," *Opt. Lett.* **16**, No. 8 (15 April 1991), 605–607.
8. J. H. Hong, I. McMichael, T. Y. Chang, W. Christian, and E. G. Paek, "Volume holographic memory systems: Techniques and architectures," *Opt. Eng.* **34**, No. 8 (August 1995), 2193–2203.
9. A. Kewitsch, M. Segev, A. Yariv, and R. R. Neurgaonkar, "Electric-field multiplexing/demultiplexing of volume holograms in photorefractive media," *Opt. Lett.* **18**, No. 7 (1 April 1993), 534–536.
10. Y. Qiao, S. Orlov, D. Psaltis, and R. R. Neurgaonkar, "Electrical fixing of photorefractive holograms in $\text{Sr}_{0.75}\text{Ba}_{0.25}\text{Nb}_2\text{O}_6$," *Opt. Lett.* **18**, No. 12 (15 June 1993), 1004–1006.
11. A. Y. Liu, M. C. Bashaw, L. Hesselink, M. Lee, and R. S. Feigelson, "Observation and thermal fixing of holographic gratings in lead barium niobate crystal," *Opt. Lett.* **22**, No. 3 (1 February 1997), 187–189.
12. D. Brady, K. Hsu, and D. Psaltis, "Periodically refreshed multiply exposed photorefractive holograms," *Opt. Lett.* **15**, No. 14 (15 July 1990), 817–819.
13. J. Otten, A. Ozols, M. Reinfeld, and K. H. Ringhofer, "Self enhancement in lithium niobate," *Opt. Lett.* **72**, No. 3, 4 (15 July 1989), 175–179.

Distribution

Admnstr
Defns Techl Info Ctr
Attn DTIC-OCP
8725 John J Kingman Rd Ste 0944
FT Belvoir VA 22060-6218

Ofc of the Dir Rsrch and Engrg
Attn R Menz
Pentagon Rm 3E1089
Washington DC 20301-3080

Ofc of the Secy of Defns
Attn ODDRE (R&AT) G Singley
Attn ODDRE (R&AT) S Gontarek
The Pentagon
Washington DC 20301-3080

OSD
Attn OUSD(A&T)/ODDDR&E(R) R Tru
Washington DC 20301-7100

CECOM
Attn PM GPS COL S Young
FT Monmouth NJ 07703

CECOM RDEC Elect System Div Dir
Attn J Niemela
FT Monmouth NJ 07703

CECOM
Sp & Terrestrial Commctn Div
Attn AMSEL-RD-ST-MC-M H Soicher
FT Monmouth NJ 07703-5203

Dir of Assessment and Eval
Attn SARD-ZD H K Fallin Jr
103 Army Pentagon Rm 2E673
Washington DC 20301-0163

Hdqtrs Dept of the Army
Attn DAMO-FDT D Schmidt
400 Army Pentagon Rm 3C514
Washington DC 20301-0460

MICOM RDEC
Attn AMSMI-RD W C McCorkle
Redstone Arsenal AL 35898-5240

US Army Avn Rsrch, Dev, & Engrg Ctr
Attn T L House
4300 Goodfellow Blvd
St Louis MO 63120-1798

US Army CECOM Rsrch, Dev, & Engrg Ctr
Attn R F Giordano
FT Monmouth NJ 07703-5201

US Army Edgewood Rsrch, Dev, & Engrg Ctr
Attn SCBRD-TD J Vervier
Aberdeen Proving Ground MD 21010-5423

US Army Info Sys Engrg Cmnd
Attn ASQB-OTD F Jenia
FT Huachuca AZ 85613-5300

US Army Materiel Sys Analysis Agency
Attn AMXSY-D J McCarthy
Aberdeen Proving Ground MD 21005-5071

US Army Matl Cmnd
Dpty CG for RDE Hdqtrs
Attn AMCRD BG Beauchamp
5001 Eisenhower Ave
Alexandria VA 22333-0001

US Army Matl Cmnd
Prin Dpty for Acquisition Hdqtrs
Attn AMCDCG-A D Adams
5001 Eisenhower Ave
Alexandria VA 22333-0001

US Army Matl Cmnd
Prin Dpty for Techlgy Hdqtrs
Attn AMCDCG-T M Fisette
5001 Eisenhower Ave
Alexandria VA 22333-0001

US Army Natick Rsrch, Dev, & Engrg Ctr
Acting Techl Dir
Attn SSCNC-T P Brandler
Natick MA 01760-5002

US Army Rsrch Ofc
Attn G Iafrate
4300 S Miami Blvd
Research Triangle Park NC 27709

US Army Simulation, Train, & Instrmntn
Cmnd
Attn J Stahl
12350 Research Parkway
Orlando FL 32826-3726

Distribution (cont'd)

US Army Tank-Automotive & Armaments
Cmnd
Vetronics Technl Ctr
Attn AMSTA-TR-R G M Bochenek MS 264
Attn AMSTA-AR-TD C Spinelli Bldg 1
Attn AMSTA-TA J Chapin
Warren Mi 48397-5000

US Army Test & Eval Cmnd
Attn R G Pollard III
Aberdeen Proving Ground MD 21005-5055

US Army Train & Doctrine Cmnd
Battle Lab Integration & Technl Dirctr
Attn ATCD-B J A Klevecz
FT Monroe VA 23651-5850

US Military Academy
Dept of Mathematical Sci
Attn MAJ D Engen
West Point NY 10996

USAASA
Attn MOAS-AI W Parron
9325 Gunston Rd Ste N319
FT Belvoir VA 22060-5582

Nav Surface Warfare Ctr
Attn Code B07 J Pennella
17320 Dahlgren Rd Bldg 1470 Rm 1101
Dahlgren VA 22448-5100

GPS Joint Prog Ofc Dir
Attn COL J Clay
2435 Vela Way Ste 1613
Los Angeles AFB CA 90245-5500

Special Assist to the Wing Cmndr
Attn 50SW/CCX Capt P H Bernstein
300 O'Malley Ave Ste 20
Falcon AFB CO 80912-3020

DARPA
Attn B Kaspar
Attn L Stotts
3701 N Fairfax Dr
Arlington VA 22203-1714

ARL Electromag Group
Attn Campus Mail Code F0250 A Tucker
University of Texas
Austin TX 78712

Univ of Arkansas Dept of Physics
Attn G Salamo
Fayetteville AR 72701

Dir for MANPRINT
Ofc of the Deputy Chief of Staff for Prsnl
Attn J Hiller
The Pentagon Rm 2C733
Washington DC 20301-0300

Natl Sci Foundation
Attn R J Anderson
4201 Wilson Blvd Ste 875
Arlington VA 22230

Palisades Instit for Rsrch Svc Inc
Attn E Carr
1745 Jefferson Davis Hwy Ste 500
Arlington VA 22202-3402

US Army Rsrch Lab
Attn AMSRL-SE-EO B Zandi
Bldg 357
FT Belvoir VA 22060

US Army Rsrch Lab
Attn J Zavada
PO Box 12211
Research Triangle Park NC 27709-2211

US Army Rsrch Lab
Attn AMSRL-CI-LL Technl Lib (3 copies)
Attn AMSRL-CS-AL-TA Mail & Records
Mgmt
Attn AMSRL-CS-AL-TP Technl Pub (3 copies)
Attn AMSRL-SE-EO A Lee
Attn AMSRL-SE-EO A Mott
Attn AMSRL-SE-EO B Ketchel
Attn AMSRL-SE-EO C Heid (20 copies)
Attn AMSRL-SE-EO C Walker
Attn AMSRL-SE-EO D Chiu

Distribution (cont'd)

US Army Rsrch Lab (cont'd)

Attn AMSRL-SE-EO D Mackie
Attn AMSRL-SE-EO D Morton
Attn AMSRL-SE-EO D Prather
Attn AMSRL-SE-EO D Robertson
Attn AMSRL-SE-EO D Smith
Attn AMSRL-SE-EO D Wilmot
Attn AMSRL-SE-EO G Daunt
Attn AMSRL-SE-EO G Euliss
Attn AMSRL-SE-EO G Wood
Attn AMSRL-SE-EO J Goff
Attn AMSRL-SE-EO J Liu
Attn AMSRL-SE-EO J Mait
Attn AMSRL-SE-EO J Pellegrino
Attn AMSRL-SE-EO J Van der Gracht
Attn AMSRL-SE-EO K Bennett
Attn AMSRL-SE-EO L Harrison

US Army Rsrch Lab (cont'd)

Attn AMSRL-SE-EO L Merkle
Attn AMSRL-SE-EO M Ferry
Attn AMSRL-SE-EO M Miller
Attn AMSRL-SE-EO N Dhar
Attn AMSRL-SE-EO N Gupta
Attn AMSRL-SE-EO P Brody
Attn AMSRL-SE-EO P Taylor
Attn AMSRL-SE-EO R Dahmani
Attn AMSRL-SE-EO S Blomquist
Attn AMSRL-SE-EO S Sarama
Attn AMSRL-SE-EO T Tayag
Attn AMSRL-SE-EO T Wong
Attn AMSRL-SE-EO W Clark
Attn AMSRL-SE-EO H Pollehn
Adelphi MD 20783-1197

REPORT DOCUMENTATION PAGE			<i>Form Approved</i> OMB No. 0704-0188	
Public reporting burden for this collection of information is estimated to average 1 hour per response, including the time for reviewing instructions, searching existing data sources, gathering and maintaining the data needed, and completing and reviewing the collection of information. Send comments regarding this burden estimate or any other aspect of this collection of information, including suggestions for reducing this burden, to Washington Headquarters Services, Directorate for Information Operations and Reports, 1215 Jefferson Davis Highway, Suite 1204, Arlington, VA 22202-4302, and to the Office of Management and Budget, Paperwork Reduction Project (0704-0188), Washington, DC 20503.				
1. AGENCY USE ONLY (Leave blank)		2. REPORT DATE February 1998	3. REPORT TYPE AND DATES COVERED Progress, from Nov. 1996 to Aug. 1997	
4. TITLE AND SUBTITLE 3-D Holographic Display Using Strontium Barium Niobate			5. FUNDING NUMBERS PE: 611102A	
6. AUTHOR(S) Christy A. Heid, Brian P. Ketchel, Gary L. Wood (ARL), Richard J. Anderson (National Science Foundation), and Gregory J. Salamo (University of Arkansas)				
7. PERFORMING ORGANIZATION NAME(S) AND ADDRESS(ES) U.S. Army Research Laboratory Attn: AMSRL-SE-EO (e-mail: cheid@arl.mil) 2800 Powder Mill Road Adelphi, MD 20783-1197			8. PERFORMING ORGANIZATION REPORT NUMBER ARL-TR-1520	
9. SPONSORING/MONITORING AGENCY NAME(S) AND ADDRESS(ES) U.S. Army Research Laboratory 2800 Powder Mill Road Adelphi, MD 20783-1197			10. SPONSORING/MONITORING AGENCY REPORT NUMBER	
11. SUPPLEMENTARY NOTES AMS code: 611102.H44 ARL PR: 8NE3AA				
12a. DISTRIBUTION/AVAILABILITY STATEMENT Approved for public release; distribution unlimited.			12b. DISTRIBUTION CODE	
13. ABSTRACT (Maximum 200 words) <p>An innovative technique for generating a three-dimensional holographic display using strontium barium niobate (SBN) is discussed. The resultant image is a hologram that can be viewed in real time over a wide perspective or field of view (FOV). The holographic image is free from system-induced aberrations and has a uniform, high quality over the entire FOV. The enhanced image quality results from using a phase-conjugate read beam generated from a second photorefractive crystal acting as a double-pumped phase-conjugate mirror (DPPCM). Multiple three-dimensional images have been stored in the crystal via wavelength multiplexing.</p>				
14. SUBJECT TERMS Hologram, 3-D display, photorefraction, phase-conjugate mirror			15. NUMBER OF PAGES 23	
			16. PRICE CODE	
17. SECURITY CLASSIFICATION OF REPORT Unclassified	18. SECURITY CLASSIFICATION OF THIS PAGE Unclassified	19. SECURITY CLASSIFICATION OF ABSTRACT Unclassified	20. LIMITATION OF ABSTRACT UL	